# Plasma Driven Permeation of Hydrogen in Tungsten Deposition Layer under Co-Deposition of Tungsten and Hydrogen

Kentaro MASUTA[1)], Kazunari KATAYAMA[2)]*

[1)] *Kyushu University, Interdisciplinary Graduate School of Engineering Science, Kasuga, Fukuoka 816-8580, Japan*
[2)] *Kyushu University, Faculty of Engineering Science, Kasuga, Fukuoka 816-8580, Japan*

(Received 25 July 2025 / Accepted 5 October 2025)

This study investigates the influence of tungsten (W) deposition on hydrogen plasma-driven permeation (PDP) behavior by examining co-deposition of W and hydrogen on a nickel (Ni) substrate. Experiments were performed using RF plasma sputtering at a substrate temperature of 693 K. The measured hydrogen permeation flux exhibited a transient peak followed by a steady-state phase, even as the W deposition layer continued to grow. Additionally, doubling the Ni substrate thickness had no effect on the steady-state flux, indicating that the permeation was limited by surface recombination processes rather than bulk diffusion. The numerical model was developed to simulate hydrogen diffusion and surface recombination processes in both the Ni substrate and the growing W layer. As W deposition changes the surface condition, the recombination coefficient ($K_r$) was expressed as a function of time, which successfully reproduced the transient peak observed in the experiment. The temporal suppression of $K_r$ was attributed to the initial deposition of W atoms on the Ni surface. Further validation through repeated discharge experiments with pre-deposited W confirmed that the initial transition from Ni to W was responsible for the peak. These results show that surface changes such as W deposition strongly affect surface recombination, thereby influencing PDP behavior.



Keywords: hydrogen permeation, tungsten, co-deposition, recombination coefficient

DOI: 10.1585/pfr.20.1405054

## 1. Introduction

In magnetic confinement fusion reactors, hydrogen isotopes are expected to permeate from the plasma through the plasma-facing wall (PFW) to the coolant side [1]. Understanding this permeation behavior is critical for improving fuel utilization and managing tritium inventories. Plasma-driven permeation (PDP), which occurs due to the bombardment of hydrogen ions and neutral particles injected from the plasma, is governed by key material parameters such as hydrogen diffusivity, solubility, recombination coefficient, trapping energy, and projected range [2]. For tungsten (W), a primary candidate for the PFW material in next-generation reactors such as DEMO, these properties have been extensively reported [3–7]. Meanwhile, observations in experimental reactors have shown that plasma–wall interactions can cause wall materials to sputter, with the resulting particles redepositing on the PFW surface to form W-containing co-deposited layers [8, 9]. Under such conditions, hydrogen isotopes and sputtered W particles simultaneously impinge on the surface, leading to concurrent deposition, hydrogen implantation, and retention. These co-deposited layers are typically characterized by high hydrogen retention, porous or defect-rich microstructures, and complex trap site distributions, which differ markedly from those of bulk W [10–12]. PDP measurements during the formation of W-H co-deposited layers have revealed that the hydrogen transport properties in these layers differ significantly from those in bulk W [13–15]. In addition, surface conditions evolve over time due to W deposition, potentially affecting surface-related parameters such as the surface recombination coefficient ($K_r$). For example, changes in surface morphology or chemical potential reduce the number of active adsorption sites, resulting in temporal variations in $K_r$. Such surface evolution effects warrant further investigation to evaluate their influence on PDP behavior.

In this study, hydrogen permeation through a metal substrate was measured under simultaneous exposure to hydrogen and W particles. Numerical modeling, which considered hydrogen diffusion and surface recombination processes, was also conducted to analyze the experimental data. These experimental and computational approaches were employed to investigate the influence of W deposition on PDP rates, with particular attention to the effects of evolving surface conditions on $K_r$.

*Corresponding author's e-mail: katayama.kazunari.947@m.kyushu-u.ac.jp

## 2. Experimental and Calculation Methods

### 2.1 Hydrogen permeation measurement

The co-deposition of hydrogen and W was performed using a plasma sputtering device. Hydrogen plasma was generated by applying a radio frequency power (200 W) to a W sputtering target in a hydrogen gas environment (40 Pa). A self-bias voltage of 800 V was applied to the W target to induce sputtering and recoil at the target by hydrogen ions. Both hydrogen and W particles are then injected onto a nickel (Ni) substrate with a diameter of 13 mm and 20 μm thickness (The Nilaco Corp., 99+% purity), as shown in Fig. 1. Ni was selected as the substrate material because it has a hydrogen permeability that is 2–3 orders of magnitude higher than that of W and its hydrogen transport parameters are well established, making it suitable for evaluating the effect of W deposition on PDP behavior. The ion flux and density at the center of the plasma measured by the Langmuir probe was $7 \times 10^{18}$ ions $m^{-2}$ $s^{-1}$ and $1.1 \times 10^{16}$ $m^{-3}$, respectively. Also, the incident energy of hydrogen particles was estimated to be 480 eV [15]. The permeated hydrogen was measured using a quadrupole mass spectrometer, calibrated with the hydrogen calibration gas (Vacuum Technology Inc.). The Ni substrate was heated by a sheath heater wrapped around the permeation flange. Substrate temperature was measured by a thermocouple in contact with the back side of the Ni substrate and controlled at 693 K by a temperature controller.

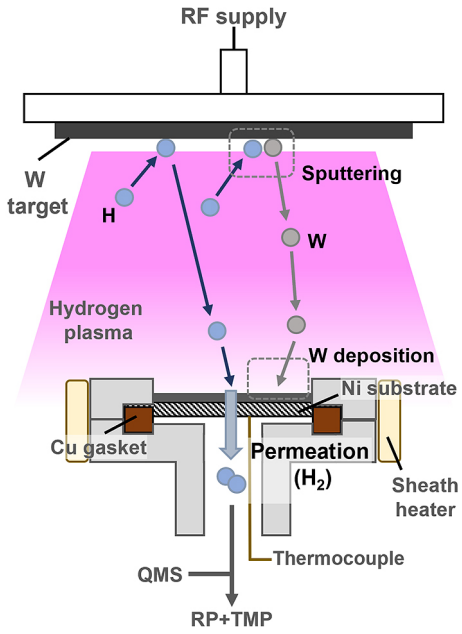


Fig. 1. Experimental setup for measuring the permeation flux under co-deposition of W sputtered particles and hydrogen on a Ni substrate (QMS: Quadrupole Mass Spectrometer, RP: Rotary Pump, TMP: Turbo Molecular Pump).

### 2.2 Calculation model for the experimental system

The modeling of hydrogen migration in a metal film was conducted in previous studies [16, 17], but the continuous increase in film thickness (as observed in our experiment) is not assumed in these models. In this paper, the calculation model suitable for our experimental system was prepared as shown in Fig. 2. In the PDP model of this study, the one-dimensional diffusion equation in the Ni substrate (Eq. (1)) and in the W deposition layer (Eq. (2)) was solved, and the permeation flux ($\Gamma_{perm}$, Eq. (3)) was calculated. It should be noted that Fig. 2 is a schematic illustration for clarity, and the thickness ratio of the Ni substrate (20 μm) and the W deposited layer (about 0.3 μm after 24 h) is not to scale.

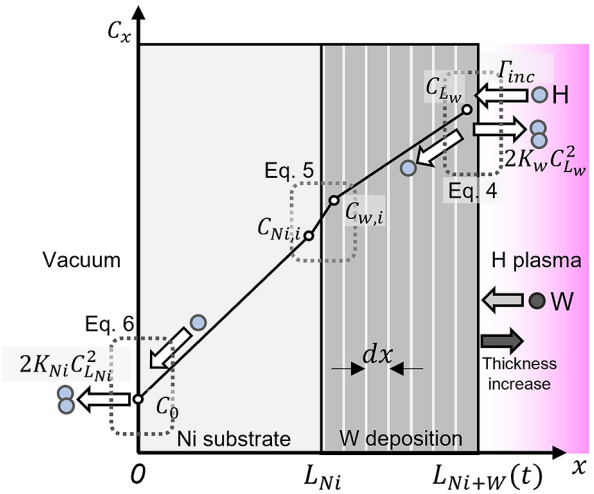


Fig. 2. Calculation model for the hydrogen permeation in the system with increasing W deposition.

$$\frac{\partial C_x}{\partial t} = \begin{cases} D_{Ni}\dfrac{\partial^2 C_x}{\partial x^2}, & 0 \le x \le L_{Ni} \quad (1) \\ D_W \dfrac{\partial^2 C_x}{\partial x^2}, & L_{Ni} \le x \le L_{Ni+W} \quad (2) \end{cases}, \tag{1}$$

$$\Gamma_{perm} = -D_{Ni}\frac{\partial C_x}{\partial x}\bigg|_{x=0}, \tag{3}$$

where $x$ is the position from the back side of substrate [m], $C_x$ is hydrogen concentration at $x$ [atom $m^{-3}$], $t$ is time [s], $D_W$ and $D_{Ni}$ are hydrogen diffusivity [$m^2$ $s^{-1}$] in W deposition layer and Ni substrate, respectively, $L_{Ni}$ represents the thickness of Ni substrate [m] and $L_{Ni+W}$ is the distance from the back side ($x = 0$) to the surface of W deposition. The boundary conditions are applied to three boundaries: plasma and surface of W deposition (Eq. (4)), W deposition and Ni substrate (Eq. (5)), and back side of Ni substrate and gas phase in the vacuum side (Eq. (6)).

$$\Gamma_{inc} = 2K_r^W C_{L_{Ni+W}}^2 - D_W \frac{\partial C_x}{\partial x}\bigg|_{x=L_{Ni+W}}, \quad x = L_{Ni+W}, \tag{4}$$

$$\frac{C_{W,i}}{S_W} = \frac{C_{Ni,i}}{S_{Ni}}, \quad x = L_{Ni}, \tag{5}$$

$$0 = 2K_r^{Ni} C_0^2 - D_{Ni}\frac{\partial C_x}{\partial x}\bigg|_{x=0}, \; x = 0\,. \tag{6}$$

Here, $\Gamma_{inc}$ is hydrogen incident flux [atom $m^{-2}$ $s^{-1}$], $K_r^{W\,or\,Ni}$ is

recombination coefficient [m$^4$ s$^{-1}$] and $S_{W\,or\,Ni}$ is hydrogen solubility [atom m$^{-3}$ Pa$^{-0.5}$] of W deposition layer or Ni substrate, respectively. Equations (4) and (6) are the mass balance equation for hydrogen and Eq. (5) based on Sieverts' law implies that the chemical potentials of hydrogen in Ni and W are equilibrated at the interface (the subscripts of $W, i$ and $Ni, i$ represent the concentration at the interface of each material). The thickness of W deposition increased with time like the experimental system, so $L_{Ni+W}$ is expressed as a function of time:

$$L_{Ni+W}(t) = L_{Ni} + v_d t, \tag{7}$$

where $v_d$ represents the deposition rate [m s$^{-1}$]. Here, $v_d$ is $3.92 \times 10^{-12}$ m s$^{-1}$ in the apparatus used in this study. According to this deposition rate, the number of the calculation cells for W deposition was increased for each time step.

## 3. Results and Discussion

### 3.1 PDP behavior at 693 K

As shown in Fig. 3, the PDP flux peaked immediately after the experiment started and reached a steady state after approximately 12 hours under co-deposition of hydrogen and W at 693 K. Previous results at other temperatures were also included for comparison [15], revealing that the PDP behavior observed in this experiment was different from that below 633 K. In a system where PDP is limited by the diffusion rate, the diffusion distance increases as the thickness of the W deposition layer increases, resulting in a continuous decrease in the permeation flux (as observed below 633 K). Therefore, the observed steady state of the permeation flux at 693 K indicates that PDP was not limited by the diffusion rate within the W deposition layer.

Figure 4 illustrates the time variation of the permeation flux at 693 K as the thickness of the Ni substrate was doubled from 20 to 40 μm. It is evident from Fig. 4 that the PDP behavior remained similar even the substrate thickness was doubled, the permeation fluxes in steady-state conditions were the same. Consequently, it was determined that the PDP rate at 693 K was independent of the diffusion rates within both the Ni substrate and the W deposition layer. This suggests that the PDP is limited by the surface recombination rate in the steady state.

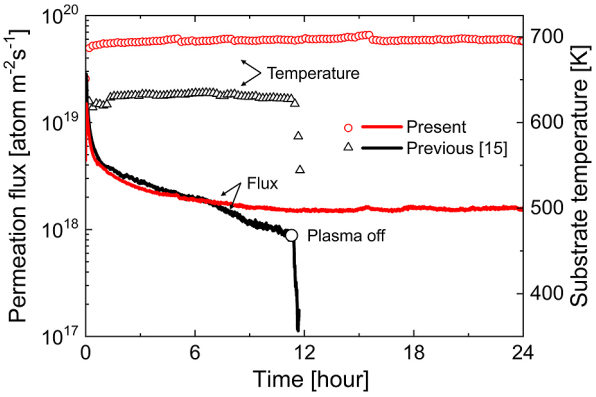


Fig. 3. Measurement result of the permeation flux at substrate temperature of 693 K. For comparison, the result of previous study is shown (633 K, discharge time 11 hours, [15]).

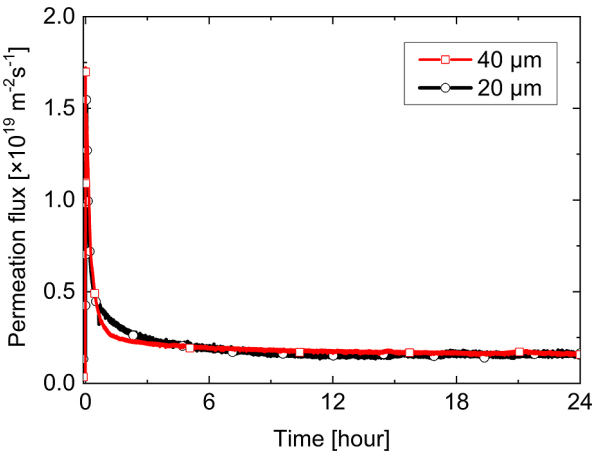


Fig. 4. Comparison of PDP flux measurements at 693 K for different Ni substrate thickness.

Table 1. Transport parameters of hydrogen at 693 K used in the calculation.

| Parameter | Value at 693 K | Ref. |
|---|---|---|
| $D_{Ni}$ [m$^2$ s$^{-1}$] | $4.66 \times 10^{-10}$ | [18] |
| $S_{Ni}$ [atom m$^{-3}$ Pa$^{-0.5}$] | $6.83 \times 10^{22}$ | |
| $K_r^{Ni}$ [m$^4$ s$^{-1}$] | $2.19 \times 10^{-27}$ | [19] |
| $D_W$ [m$^2$ s$^{-1}$] | $7.45 \times 10^{-16}$ | [13] |
| $S_W$ [atom m$^{-3}$ Pa$^{-0.5}$] | $1.83 \times 10^{26}$ | |
| $K_r^W$ [m$^4$ s$^{-1}$] | $1.05 \times 10^{-28}$ | [14] |

### 3.2 Calculation result

#### 3.2.1 Calculation parameters

The parameters required for the calculations are summarized in Table 1. Hydrogen incident on the Ni substrate consisted of ions and neutral particles, and their incident flux ($\Gamma_{inc}$) was difficult to measure directly, thus it was estimated as follows. According to experimental results, PDP flux at the substrate temperature of 693 K was limited by the hydrogen recombination rate on the incident and permeation surfaces (RR-regime). In the RR-regime at steady state, the permeation flux ($\Gamma_{perm}$ [atom m$^{-2}$ s$^{-1}$]) can be expressed by the following equation [16]:

$$\Gamma_{perm} = \frac{K_r^p}{K_r^p + K_r^i} \Gamma_{inc}, \tag{8}$$

where $K_r^{i\,or\,p}$ is the recombination coefficient on the incident or permeation side [m$^4$ s$^{-1}$] and $\Gamma_{inc}$ is the hydrogen incident flux [atom m$^{-2}$ s$^{-1}$]. In the experiment, since the value of $\Gamma_{perm}$ was $1.59 \times 10^{18}$ atom m$^{-2}$ s$^{-1}$, $K_r^i = K_r^W$ and $K_r^p = K_r^{Ni}$, then $\Gamma_{inc}$ was estimated to be $1.67 \times 10^{18}$ atom m$^{-2}$ s$^{-1}$.

#### 3.2.2 Simulation of experimental results

The PDP flux at 693 K was numerically calculated based on the model described in Sec. 2.2 using the parameters

listed in Sec. 3.2.1. As shown in Fig. 5, the calculated result assuming a constant recombination coefficient of W ($K_r^W$) on the incident side (denoted as Calc. 1) fails to capture the transient peak observed in the experimental data. This discrepancy is considered to arise from the assumption that $K_r$ remains constant throughout the process, despite the surface being composed of Ni in the initial stage.

$K_r$ is well known to be highly sensitive not only to material composition and temperature but also to surface conditions such as contamination, oxidation, and morphology [20]. In particular, non-hydrogen impurities can increase the surface potential barrier or occupy adsorption/desorption sites, thereby suppressing the recombination process and reducing $K_r$. It has been reported that the recombination coefficient decreases by 2 to 3 orders of magnitude due to the presence of $H_2O$ and $D_2O$ on type 304 stainless steel surfaces [21], and sulfur contamination on Ni surfaces [22]. Based on these findings, it is reasonable to assume that in the present experiment, $K_r$ was significantly reduced immediately after plasma ignition due to the adherence of W atoms to the Ni surface, and gradually approached the value corresponding to the fully developed W deposition layer as the surface evolved. To account for these changes in the surface condition, $K_r$ was treated as a variable parameter, and numerical simulations were performed accordingly (denoted as Calc. 2). In this model, the temporal evolution of $K_r$ was defined by the following piecewise function:

$$K_r(t) = \begin{cases} K_r^{Ni} + \left(K_r^{min} - K_r^{Ni}\right)\dfrac{t}{t_1}, \\ \quad t < t_1 \\ K_r^{min} + \left(K_r^{W} - K_r^{min}\right)\left(1 - \exp\left(-\dfrac{t - t_1}{\tau}\right)\right), \\ \quad t \geq t_1 \end{cases}, \quad (9)$$

where $K_r^{Ni}$ is the recombination coefficient corresponding to the bare Ni surface, $K_r^W$ is the steady-state value for the fully developed W deposition layer, $K_r^{min}$ is the minimum recombination coefficient during the transition, and $\tau$ is the time constant representing the recovery rate of $K_r$. The parameters $K_r^{min}$ and $\tau$ were optimized to minimize the error between the calculated and experimental permeation fluxes. The parameter $t_1$ represents the time at which $K_r$ reaches $K_r^{min}$, marking the transition from the initial linear decline phase to the exponential recovery phase. This transition time coincides with the onset of the permeation rise observed in the experiment, which occurred at $t_1 = 20$ s. The resulting fit, shown as Calc. 2 in Fig. 5, successfully reproduced the transient peak behavior observed in the experiment (optimized parameters were $K_{min} = 4.2 \times 10^{-31}$ m$^4$ s$^{-1}$ and $\tau = 4.5 \times 10^3$ s).

Figure 6 compares the time evolution of the hydrogen concentration at the outermost surface under two conditions: one with the recombination coefficient at the plasma side fixed at a constant value ($K_r = K_r^W$), and the other with $K_r$ expressed as a function of time as defined by Eq. (9). The result clearly shows that the suppression of surface recombination due to the reduced $K_r$ leads to a sharp increase in surface hydrogen concentration. This elevated concentration enhances hydrogen diffusion toward the permeation side, which is considered to have caused the transient peak in the permeation flux.

### 3.2.3 Experimental validation of peak behavior

Based on the permeation calculation presented in the previous section, the transient increase in permeation flux and the appearance of a peak were attributed to W deposition on the Ni surface and the resulting temporary decrease in $K_r$. To experimentally verify this hypothesis, plasma discharges were applied for 1,000 seconds to pre-deposit W onto the Ni surface, followed by permeation measurements. This discharge-and-pause cycle was repeated three times, during which the permeation behavior was observed.

As shown in Fig. 7, a sharp peak in the permeation flux was observed only during the first plasma discharge, whereas no such peaks appeared in the second and third discharges. This result confirms that the initial transition of the incident

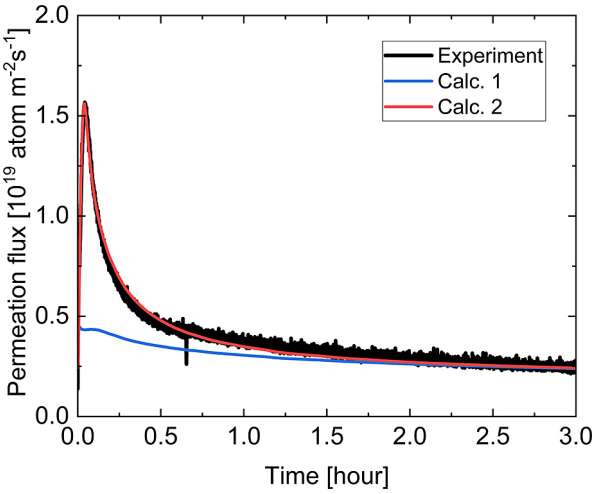


Fig. 5. Comparison of calculation with the experiment result (Calc. 1: $K_r$ is constant at $K_r^W$, Calc. 2: $K_r$ is changed as Eq. (9)).

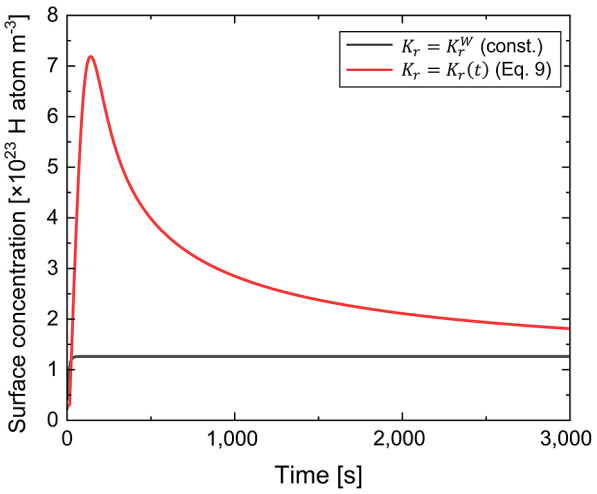


Fig. 6. Time evolution of surface hydrogen concentration with $K_r$ fixed at $K_r^W$ and $K_r$ expressed as the function of time (Eq. (9)).

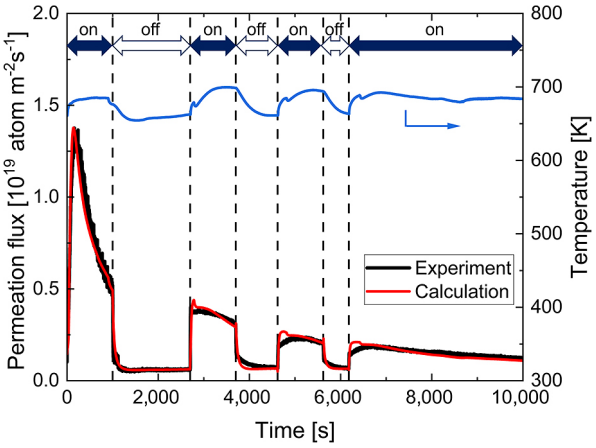


Fig. 7. Permeation flux during repeated plasma discharges; "on" and "off" denote discharge and shutdown periods, respectively.

surface from Ni to W plays a significant role in producing the transient peak in the permeation flux. Furthermore, numerical simulations incorporating $K_r$ expressed as a function of time, as described in the previous section, were conducted. In the simulations, $K_r$ was held constant during the plasma-off periods, the incident flux ($\Gamma_{inc}$ in Eq. (4)) was set to zero, and the W film thickness was kept unchanged. The simulation results were generally consistent with the experimental data, except for the deviation in the permeation response just after plasma ignition. This difference is considered to be caused by a temperature rise of approximately 30 K at each plasma ignition due to heat loading, which led to an increase in $K_r$, enhanced surface recombination on the plasma side, and consequently, suppression of permeation. Since the current model with $K_r$ expressed as a function of time does not respond to localized temperature variations, it is likely that $K_r$ was underestimated in the simulation, resulting in an overestimation of the initial rise in the permeation flux.

## 4. Conclusion

PDP behavior of hydrogen was investigated at 693 K under co-deposition conditions of hydrogen and W onto a Ni substrate. The PDP flux exhibited a transient peak followed by a steady state, even as the W deposition continued to grow. Furthermore, doubling the thickness of the Ni substrate had no effect on the steady-state flux, indicating that permeation was not limited by bulk diffusion, but rather by surface recombination processes under steady-state conditions. Numerical simulations incorporating $K_r$ expressed as a function of time successfully reproduced the transient peak observed in the experiment. This was achieved by modeling $K_r$ as being initially suppressed due to the adherence of W to the Ni surface and gradually recovering to the intrinsic value for W. Experimental validation using repeated plasma discharge cycles with pre-deposited W confirmed that the transient peak occurred only during the initial transition from Ni to W. Based on the above results, the temporal variation of $K_r$ on the plasma-facing surface is considered to have a direct influence on PDP behavior. Therefore, in fusion reactors, $K_r$ and the PDP rate are expected to vary with the changes in surface condition caused by W deposition. As demonstrated in this study, the formation of a W deposition layer leads to a temporary variation in $K_r$ and a corresponding change in permeation, but $K_r$ eventually converges to the intrinsic value for W deposition layer, resulting in a stabilization of the PDP behavior.

## Acknowledgment

This work was supported by JSPS KAKENHI Grant Number JP25KJ1938.

[1] K. Katayama *et al.*, Fusion Eng. Des. **169**, 112576 (2021).
[2] O.V. Ogorodnikova, J. Nucl. Mater. **277**, 130 (2000).
[3] R.A. Anderl *et al.*, J. Nucl. Mater. **212–215**, 1416 (1994).
[4] R.A. Causey and T.J. Venhaus, Phys. Scr. **T94**, 9 (2001).
[5] T. Tanabe, Phys. Scr. **T159**, 014044 (2014).
[6] H.D. Liu *et al.*, Fusion Eng. Des. **148**, 111267 (2019).
[7] M. Zhao *et al.*, Fusion Eng. Des. **160**, 111853 (2020).
[8] M. Rasinski *et al.*, Fusion Eng. Des. **86**, 1753 (2011).
[9] A. Baron-Wiechec *et al.*, J. Nucl. Mater. **463**, 157 (2015).
[10] G. De Temmerman and R.P. Doerner, J. Nucl. Mater. **389**, 479 (2009).
[11] S. Krat *et al.*, Vacuum **149**, 23 (2018).
[12] M.J. Baldwin *et al.*, Nucl. Mater. Eng. **23**, 100743 (2020).
[13] Y. Hara *et al.*, Fusion Eng. Des. **172**, 112851 (2021).
[14] Y. Xu and Y. Hirooka, Nucl. Fusion **58**, 076005 (2018).
[15] K. Masuta *et al.*, Fusion Sci. Eng. **80**, 540 (2024).
[16] B.L. Doyle, J. Nucl. Mater. **111–112**, 628 (1982).
[17] G.R. Longhurst, TMAP7 User Manual, 2008.
[18] W.M. Robertson, Julich-Conf. **II**, 449 (1972).
[19] M.I. Baskes, J. Nucl. Mater. **92**, 318 (1980).
[20] M.A. Pick and K. Sonnenberg, J. Nucl. Mater. **131**, 208 (1985).
[21] M. Takizawa *et al.*, J. Nucl. Mater. **248**, 15 (1997).
[22] M. Yamawaki *et al.*, J. Nucl. Mater. **162–164**, 1071 (1989).